BETA-DELAYED PARTICLE EMISSION FROM NEUTRON-DEFICIENT ISOTOPES IN THE Z~50 REGION.

P. Tidemand-Petersson *), R. Kirchner, O. Klepper and E. Roeckl
GSI-Darmstadt, D-6100 Darmstadt, Federal Republic of Germany

A. Piochocki and J. Żylicz
Institute of Experimental Physics, University of Warsaw, PL-00-681 Warsaw, Poland

D. Schardt
EP Division, CERN, CH-1211 Geneva 23, Switzerland

Abstract

Experimental studies of beta-delayed proton and alpha-particle emission from precursors in the region close to the double shell closure at N = Z = 50 are described. The results range from identification of new precursors like ^{96}Ag and ^{103}, ^{105}Sn, to determination of branching ratios, feeding of excited levels after particle emission and the energy available for proton emission. Comparison of the results with statistical-model calculations points to a resonance in the beta-strength function in the decay of ^{110,112}I, ^{113}Xe, ^{114,116}Cs and ^{117}Ba.

1. Introduction

The evolution since the first observation of beta-delayed proton emission [1, 2] has made it clear that this decay mode is characteristic for very neutron-deficient nuclides of many elements. The combination of large beta-decay energies and small binding energies of charged particles in such nuclides permits also other decay modes as shown by the example of ^{110}I in Fig. 1. However, of the beta-delayed decay channels which - at least in principle - are open for this nucleus, only two have been observed so far: the emission of protons and alpha particles from the excited levels fed by beta decay.

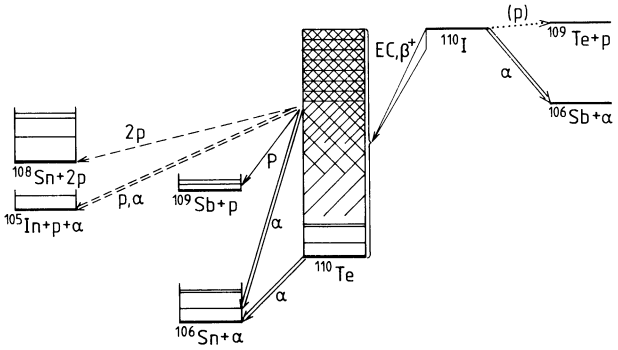

Fig. 1 Schematic presentation of possible decay modes of the T_z = 2 nuclide ^{110}I. The nuclear masses were taken from the droplet-model calculations by Myers (in ref. 3). Note the many channels open for particle emission following beta-decay of ^{110}I to excited levels in ^{110}Te: In addition to proton and alpha decay, emission of two protons, a proton plus an alpha particle, and even of ^{3}He becomes energetically possible (the latter decay mode is omitted in the figure for simplicity). Decay channels already identified are shown as full-drawn lines, while so far unobserved modes are given as dashed lines.

Along with the identification of ever more particle precursors, the investigations of these precursors have changed character from being studies of an exotic decay mode as such, into applications of this decay channel to obtain information on nuclear properties. In the following we present examples from the region Z ~ 50 of both identification of new particle precursors and more thoroughly studies of selected precursors. The latter should be seen as an attempt to perform rather "complete" experiments in the sense of measuring as many decay properties as possible, in order to approach a unique determination of the numerous parameters used in the theoretical description of the process. The identification of new precursors includes e.g. the so far lightest known isotopes of tin (Z = 50) and a series of N = 49 precursors. The applications have mainly been performed for precursors with 53 ≤ Z ≤ 56 and the interest has been focussed on the derivation of information on masses [4] and the beta-strength function [5-8], but includes also the first observation of an earlier unknown excited nuclear level by means of coincidence measurements of beta-delayed alpha particles and γ-rays.

2. Experimental techniques

As mentioned above, the particle precursors are characterized by their remoteness from the region of stable and long-lived nuclides. Unfortunately this means in most cases that the cross-section for formation of such a nuclide is only a small fraction of the total reaction cross-section. This makes an isolation of one or a few nuclides from the rest of the reaction products a necessary condition in order to allow for subsequent spectroscopic investigations. The most powerful tool for this selection has proven to be on-line mass separation.

The experiments presented in the following have all been performed at the GSI mass separator [9] on-line to the heavy-ion accelerator UNILAC. The activity was produced as evaporation residues by bombardment of 2 - 4 mg/cm^2 targets of ^{50}Cr, ^{54}Fe, $^{58, 60}$Ni and 63, ^{65}Cu with 4 - 5 MeV/u ions of 15 - 40 particle-nA (pnA) beams of ^{40}Ca and ^{58}Ni. The recoiling products were stopped in the catcher foil of an ion source [10], ionized, extracted and accelerated by a voltage difference of 50 kV. They were then sorted according to their masses by the magnetic field of the separator, and the beam corresponding to the selected mass was directed to the actual collection position.

*) Present address : II. Physikalisches Institut, Universität Göttingen, D-3400 Göttingen Federal Republic of Germany.

In the present investigations three measuring positions were used: by means of two sets of electrostatic deflector plates, two mass-separated beams could simultaneously be guided to and stopped in two 10 $\mu g/cm^2$ thick carbon foils, each situated on a wheel equipped with two such foils, a calibration alpha source and a light-screen for beam adjustments. Behind the wheel a telescope, consisting of a 21 - 29 µm thick and 150 mm^2 large energy-loss (ΔE) and a ~700 µm thick, 450 mm^2 large rest-energy (E) surface-barrier silicon detectors, were recording the particles emitted from the sources collected in the carbon foils. An additional calibration source for the E-detector was placed on a second wheel behind the telescope, so that both detectors could be calibrated without breaking the vacuum. Alternatively a third mass could be implanted into the aluminized mylar tape of a fast tape-transport system, which at pre-selected intervals brought the activity to a measuring position 30 cm away from the collection position. This measuring position was also equipped with a detector telescope and calibration sources placed on vertical bars. In addition to the SB-detectors also beta-detectors (1 mm thick scintillators) and/or photon-detectors (Ge(Li) or intrinsic Ge) could be placed at the measuring positions, thus allowing for recording of particle-beta, particle-gamma and particle-X-ray coincidences.

The data were recorded event-by-event on magnetic tape by a PDP 11/45 computer system. In the subsequent data analysis various gate-settings allowed sorting of the data according to particle type (alpha, beta or proton) and energy of particle and photon.

3. Identification of new particle precursors and determination of new decay properties of previously known nuclides.

The area of the nuclear chart investigated in the present series of experiments is shown in fig. 2.

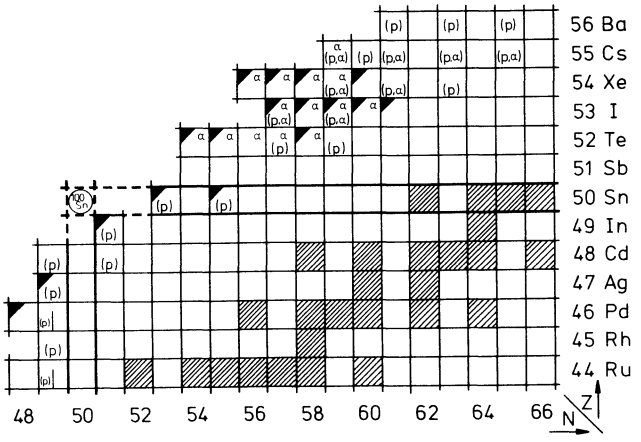

Fig. 2 Part of the chart of nuclides showing the mass regions under investigation in the present work. Beta-delayed particle precursors are indicated by the symbols of the observed particles in parentheses, while ground-state alpha decay is shown without parenthesis. The filled triangles mark nuclides whose first identification took place at the GSI on-line mass separator, while the hatched areas show the stable nuclides.

In the following, the new isotopes and properties determined are presented; the precursors are divided into separated sections by their positions on the nuclear chart.

3.1 Precursors with Z < 50

The precursors lying below tin were all produced in ^{40}Ca-induced fusion reactions in a recent survey experiment[11]. In addition to a verification of the A = 95 assignment of the beta-delayed proton activity reported[12] for ^{95m}Pd, we observed beta-delayed protons at the masses 94, 96, 97 and 100. From considerations including predicted masses[3], formation cross sections and the odd-N property of most known[13] precursors, the proton activities observed at these mass numbers were assigned to $^{94(m)}Rh$, ^{96}Ag, ^{97}Cd and ^{100}In. Of these nuclides only ^{97}Cd has earlier been identified[14] as proton precursor.

Because of the very weak activity at the masses 94 and 100, no half-life could be determined for these precursors. The half-life observed for the A = 95 activity agreed well with the 14 s reported[12] for the ^{95m}Pd precursor. For the half-life determinations for the proton activities at the masses 97 and 96 two different methods were applied: recording of pure decay curves by means of the tape-transport system, and of grow-in and decay curves by means of periodic electrostatic deflection of the mass-separated beams, which were directed to the carbon foils. In both cases the time dependence of the activity was recorded by application of a time-to-digital converter, which was started by an "end-of-transport/deflection" signal and stopped by the occurrence of a particle in the detector telescope. The decay curve for ^{97}Cd and the grow-in and decay curve of ^{96}Ag are shown as examples in figs. 3 and 4, respectively, and the half-lives determined for

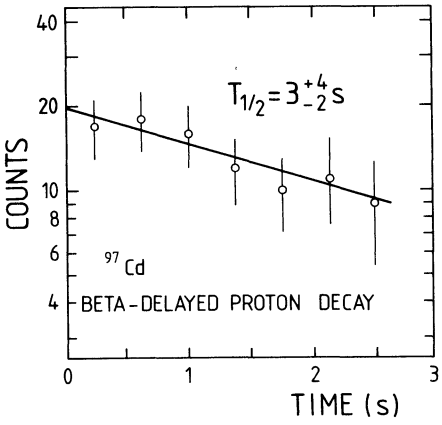

Fig. 3 Decay curve recorded for the beta-delayed proton activity observed at A = 97 and assigned to ^{97}Cd. The activity was produced by the ^{60}Ni (^{40}Ca,3n) reaction and collected at the tape-transport system which was operated with a collection time of 2.8 s.

the precursors treated in this and the following sections are given in table 1.

With the exception of ^{100}In, all the precursors treated in this section have N = 49, i.e. the corresponding proton emitters are lying on the N = 50 closed neutron shell, and the proton spectra are, therefore, expected to show peak structure induced by fluctuation phenomena[7,14] originating in the relatively low

level density. A study of this property has to wait for more detailed experiments in this region.

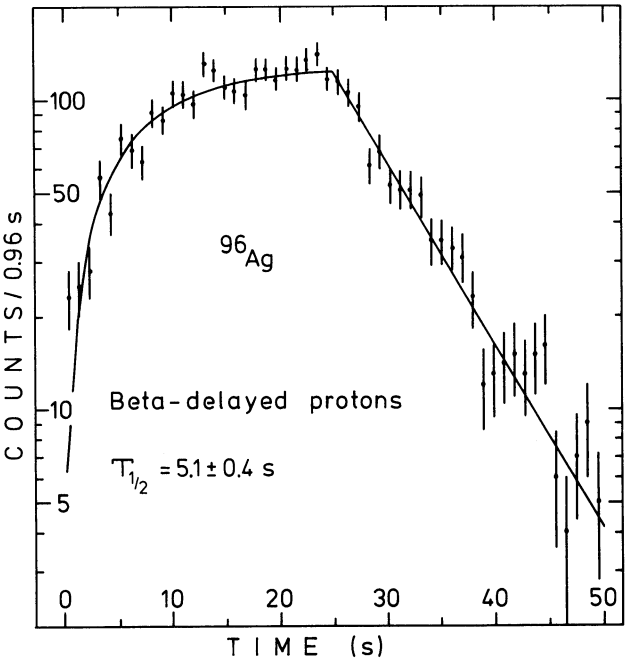

Fig. 4 Grow-in and decay curve recorded for the A = 96 proton activity simultaneously with the curve in Fig. 3. The time spectrum was obtained by means of the electrostatic deflection system operated with a collection time of 25 s.

Table 1

Half-lives of proton precursors with Z ≦ 50

Nuclide	$T_{1/2}$ (s)
^{96}Ag	5.1 ± 0.4
^{97}Cd	3 $^{+4}_{-2}$
^{103}Sn	7 ± 3
^{105}Sn	31 ± 6

3.2 New tin isotopes

The expected double magicity of ^{100}Sn has attracted much interest to the very neutron-deficient isotopes of tin and the neighbouring elements. Since the elements lighter than tellurium (Z = 52) are not expected to show alpha decay, the beta-delayed proton channel was supposed to offer the best possibility for identification of very light tin isotopes. In analogy, the fusion reactions between ^{58}Ni projectiles and ^{50}Cr or ^{54}Fe targets appeared from production cross-sections calculated using the HIVAP code [15], to be favourable for the production of such nuclides.

We have therefore applied these techniques to look for tin isotopes [16] at the mass settings A = 105, 103 and 101 of the mass separator. While for A = 105 and 103 the intensity sufficed to reach proton spectra containing some hundred counts, the spectrum recorded for A = 103 and the corresponding decay curve are shown as examples in fig. 5, only

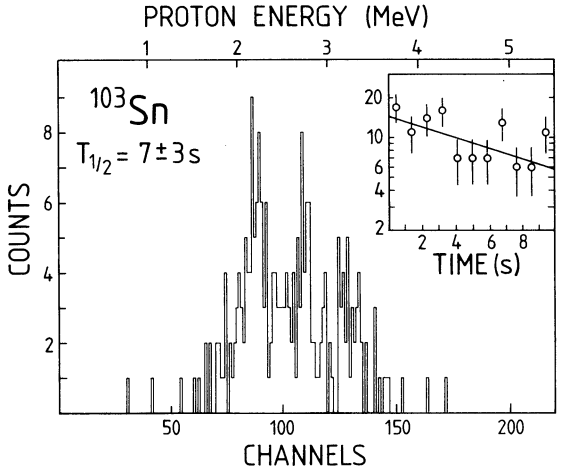

Fig. 5 Energy spectrum of the beta-delayed protons from the precursor ^{103}Sn, produced by the ^{50}Cr (^{58}Ni, 2p 3n) reaction. The decay curve shown as an inset resulted from a measurement with the tape-transport system operated with a collection time of 10 s.

15 ΔE-E coincidences of proton character were observed from the A = 101 activity. Furthermore, in contrast to the heavier masses, where the mass setting of the separator and considerations involving the compound nucleus and masses of the nuclides produced in the reactions, make an unambiguous assignment of the activity to ^{103}Sn and ^{105}Sn possible, no firm statement is possible for the A = 101 activity, and hence it cannot be claimed, that ^{101}Sn has been observed. The observed half-lives of ^{103,105}Sn (see table 1), agree qualitatively with the values of 5 s and 30 s, respectively, predicted from the gross theory of beta decay [17].

3.3 Precursors with 50 < Z ≦ 56

All precursors investigated in this element range had earlier been observed either as alpha-decaying nuclides [18-20] or as beta-delayed particle precursors. They are consequently not treated here, but in the section, where the properties determined for the individual nuclides are the main subject.

4. Determination of branching ratios

Since the determination of total particle branching ratios, i.e. the fraction of decays which is followed by emission of beta-delayed particles, and of feeding of excited levels by the emission of such particles, are rather different, they are treated separately in the following. Common for both properties is the applicability of the results in the comparison of experimental and calculated values, which is treated as well.

4.1 Beta-delayed particle branching ratios.

The main technique applied to determine the total particle branching ratio, is the comparison of intensities of beta-delayed particles and ground-state alpha particles observed with the same detection system for nuclides whose alpha-decay branch was known from earlier studies. However, also simultaneous recording of beta activity in a multiscaling mode and of beta-delayed particles has been applied [21]. The branching ratios determined in the course of the

Table 2

Half-lives and particle branching ratios for precursors with $52 \leq Z \leq 55$

Precursor	$T_{1/2}$ (s)	$P_{d.p.}$ [a]	$P_{d.\alpha}$ [a]	$P_{d.p.}/P_{d.\alpha}$
^{108}Te	2.1 ± 0.1 [b]	0.05 ± 0.02	-	
^{109}Te	4.1 ± 0.2 [c]	$(9.2 \pm 3.1)\cdot10^{-2}$	-	
^{110}I	0.65 ± 0.02 [d]	0.11 ± 0.04	$(1.1 \pm 0.4)\cdot10^{-2}$	10.2 ± 0.7
^{112}I	3.42 ± 0.11 [c]	+	+	8.5 ± 0.2
^{113}Xe	2.78 ± 0.15 [e]	+	+	750 ± 150 [e]
^{114}Cs	0.57 ± 0.02 [f]	0.07 ± 0.02 [f]	$(1.6 \pm 0.6)\cdot10^{-3}$ [f]	45.5 ± 1.2

a) A "+" in this column means that this kind of activity was observed, but the branching ratio was not determined, whereas a "-" indicates that no such activity was observed.

b) From ref.[18] c) from ref.[22] d) from ref.[19]

e) Preliminary results from recent measurements. More accurate values are expected to result from the final analysis.

f) from ref.[21]

present studies are summarized along with the half-lives in table 2 and in addition they are treated individually in the following.

4.1.1 The nuclide ^{108}Te

has earlier been observed by its alpha decay [18,23]. Due to improvements in the production rate also a beta-delayed proton branch could be observed, and the branching ratio of $P_{d.p.} = 0.05 \pm 0.02$ could be obtained via the known [18] alpha-decay branching ratio. The relatively large error arises from a correction of the proton rate caused by contamination from the more abundant ^{109}Te.

4.1.2 The nuclide ^{109}Te

has been studied [23-25] for as well alpha decay as beta-delayed proton decay by the Dubna group. Using an improved alpha-branching ratio [19] we have in addition derived the proton-branching ratio $P_{d.p.} = (9.2 \pm 3.1)\cdot10^{-2}$.

4.1.3 The nuclide ^{110}I

was identified by its alpha decay and emission of beta-delayed protons in the early stage [22] of the present work. Using the more intense ^{110}I and ^{114}Cs activities now available, we have also observed beta-delayed alpha particles from ^{110}I and determined its alpha-decay branching ratio [19] from the $^{114}Cs \xrightarrow{\alpha} {}^{110}I \xrightarrow{\alpha} {}^{106}Sb$ decay sequence. From this value, the beta-delayed particle branching ratios were deduced to be $P_{d.p.} = 0.11 \pm 0.04$ and $P_{d.\alpha} = (1.1 \pm 0.4)\cdot10^{-2}$. The intensity for all three decay modes sufficed to record the decay curves shown in fig. 6. The three half-lives are seen to agree within an average value of $T_{1/2} = 0.65 \pm 0.02$ s.

In a 25-h experiment primarily designed to investigate the alpha-decay sequence $^{110}Xe \xrightarrow{\alpha} {}^{106}Te \xrightarrow{\alpha} {}^{102}Sn$ [19,20], we also searched for beta-delayed emission of two protons or a proton and an alpha particle from the precursor ^{110}I. For this purpose charged-particle coincidence events recorded in a detector telescope and a 50 µm thick annular detector [19] within an 8 µs time window were sorted out.

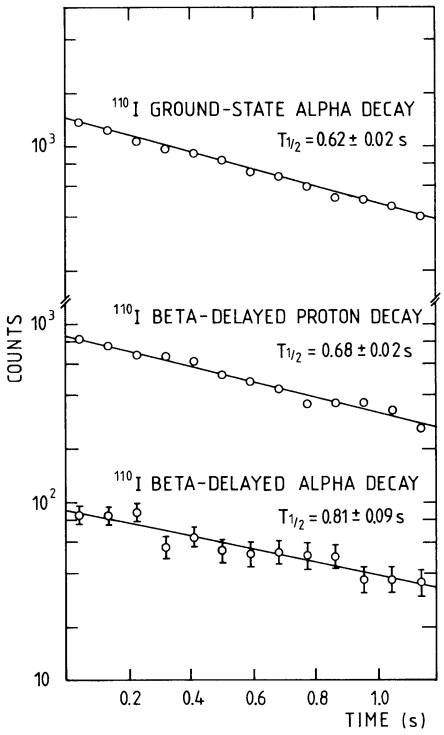

Fig. 6 Decay curves for ground-state alpha particles and beta-delayed protons and alpha particles from the ^{110}I decay. The experimental data origine from a measurement at a windmill system (collection time 1.2 s, transport time 0.2 s). In analogy with the preceding figures also least-squares fits are shown.

A few coincidences of proton-proton signature were found, but the explanation as random coincidences or positron-proton coincidences cannot be ruled out. From the number of beta-delayed proton events detected with the telescope ($7\cdot10^4$), its detection efficiency (12 % of 4π sr) and the branching ratio for this pro-

cess, an upper limit for beta-delayed two-proton emission can be deduced if an assumption is made on the proton-proton angular correlation: a 180° correlation, e.g., would correspond to a branching-ratio limit of $P_{d.2p.} \leq 8 \cdot 10^{-6}$.

4.1.4 The nuclide ^{112}I

could originally not be unambiguously identified as beta-delayed particle precursor, since ^{112}I and ^{112}Xe are both possible precursors, judged from mass predictions [3]. We have, therefore, recorded an X-ray spectrum in coincidence with the beta-delayed particles observed at this mass number. Since this spectrum showed only antimony X-rays, the activity was assigned to ^{112}I. The ratio between beta-delayed protons and alpha particles was determined to be $P_{d.p.}/P_{d.\alpha} = 8.5 \pm 0.2$.

4.1.5 The nuclide ^{114}Cs

has been subject of a recent publication [21]. Suffice it therefore here to mention that the beta-delayed particle branches, as given in table 2, were determined from a combination of beta and particle detection [21].

4.2 Feeding of excited levels by particle emission.

The addition of a Ge(Li) detector to the telescope set-ups made it possible to measure particle-gamma coincidences, yielding information on the population of excited levels by the emission of beta-delayed particles. We have performed such measurements for the two precursors treated below. The results obtained are summarized in table 3.

4.2.1 The decay of ^{113}Xe

leads after emission of protons to ^{112}Te, in which nuclide the three lowest-lying excited levels are known [26] with spin, parity and excitation energy. The relevant part of the gamma-ray spectrum recorded in coincidence with beta-delayed protons from ^{113}Xe is shown in fig. 7 together with a simplified decay scheme, showing the intensities of the individual proton transitions. The intensity of the transition leading directly to the ground state of ^{112}Te has been determined on the assumption that the four transitions shown represent essentially the total proton-decay branch. From comparisons with branching ratios calculated using the statistical model [6,7] it was found, that only the assumption of $I = 5/2$ for ^{113}Xe yielded satisfactory agreement. Based on the available orbitals for $N = 59$, it is therefore suggested that ^{113}Xe has $I = 5/2^+$.

4.2.2 The decay of ^{114}Cs

leads after particle emission to the nuclides ^{113}I and ^{110}Te for beta-delayed protons and alpha particles, respectively. In both of these nuclides no information on excited levels is available. The proton-coincident gamma lines given in table 3 can consequently not be converted into feeding of excited levels. An additional difficulty here is, that the multipolarities and hence the internal conversion coefficients are not known for these transi-

Table 3

Results of measurements of coincidences between beta-delayed particles and gamma rays for ^{113}Xe and ^{114}Cs.

Precursor	Particle emitted	Energy[a] and intensity[b] of particle-coincident γ-ray	Energy of level fed by particle emission
^{113}Xe	proton	689 keV , (53 ± 5)%	689 keV
		787 keV , (3.8 ± 0.7)%	1476 keV
		795 keV , (3.3 ± 0.6)%	1484 keV
^{114}Cs	proton[d]	121 keV , (11.8 ± 1.2)%	c)
		239 keV , (7.6 ± 0.8)%	c)
		400 keV , (3.2 ± 0.8)%	c)
		403 keV , (3.9 ± 1.0)%	c)
	alpha	656 keV , (17 ± 8)%	656 keV

a) The uncertainty of the γ-ray energies is approximately ± 1 keV.

b) The intensity is given as the fraction of particle emissions which is followed by this γ-ray.

c) Not determined

d) In addition to the γ-rays given here, a 31 keV line was assigned to follow beta-delayed proton emission from ^{114}Cs in an earlier γ-ray experiment [21]. From the relative intensities of this line and the 121 keV line it is inferred, that (14.4 ± 4.3)% of the proton emissions are followed by the 31 keV γ-ray.

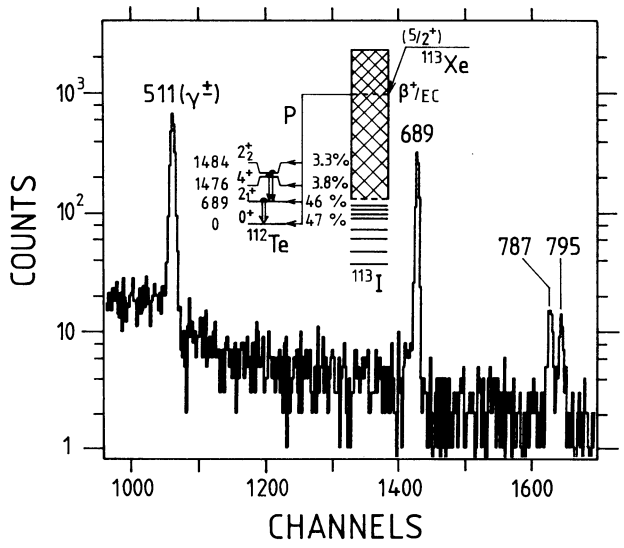

Fig. 7 Gamma-ray spectrum recorded in coincidence with beta-delayed protons from ^{113}Xe. The inset shows a simplified decay scheme for the beta-delayed proton-emission process for this precursor.

tions, so not even an assumption of the gamma-ray energies being directly representative of excited-level energies (this could well be so, since no sum of two gamma-ray energies is yielding a third energy) would make a deduction of proton-branch intensities possible.

The gamma-ray spectrum recorded in coincidence with beta-delayed alpha particles showed, in addition to the 511 keV annihilation-radiation line, only a line at 656 keV. Based on energy systematics [26,27] of 2^+ levels of even tellurium isotopes, it is almost certain that this gamma line represents the $2^+ \rightarrow 0^+$ transition in ^{110}Te. This is the first application of coincidences between beta-delayed alpha particles and gamma rays to identify a new level, and it makes it possible to follow the 2^+-level systematics until N = 58 for tellurium. It should finally be noted, that the intensity of the line corresponds to a feeding of 17 ± 8 % of the 2^+ state, a value which in analogy to the gamma-ray data [21] supports a 1^+ -assignment for ^{114}Cs, when compared with statistical-model calculations.

5. Determination of $Q_{EC} - B_p$ values

The technique applied for measurements of Q_{EC}-B_p values, i.e. the energy available for beta-delayed proton emission, is the one introduced for ^{109,111}Te by the Dubna group [25,28], namely simultaneous recording of proton spectra in singles and in coincidence with positrons. The experiments were performed at the tape station, where the measuring position was equipped with a particle-detector telescope and a 1 mm thick plastic scintillator for beta-particle detection. The two detection systems were placed face-to-face with the tape carrying the activity located between them. This secured that no contribution was added to the proton signal, when a coincident event was recorded. But for the singles proton spectrum a correction had to be performed, since a fraction of the protons, equal to the solid angle of the detector telescope (12% of 4π sr) multiplied by the $\beta^+/(EC + \beta^+)$ probability ratio for the beta transition preceding the proton emission, was shifted to an energy approximately 300 keV (the energy loss of 1 - 6 MeV positrons in the detector telescope) higher than the true energy of the proton itself, since this fraction of the protons accidentally was recorded coincident with the positron emitted in the preceding beta decay. Since this correction depends on the ratio $\beta^+/(EC + \beta^+)$, which is a function of the available energy, i.e. the quantity which is to be determined by the measurement, such corrections had to be performed in an iterative way. The correction has also been taken into account in the determination of the precision of the derived energy values.

The measurement of the Q-value for the positron decay [29] of ^{109}Sb and the available Q_α-values [19,20] in the trans-tin region, made it possible to determine the masses of three nuclides [4] lying at or very near the proton drip line by a measurement of the $Q_{EC} - B_p$ value for ^{114}Cs. For this reason and in order to approach the "complete" description of a few cases of beta-delayed particle emission, we have performed $Q_{EC} - B_p$ determinations for ^{114}Cs and ^{113}Xe.

The resulting ratios of ß-coincident and total proton intensities are shown as a function of the proton energy for these two precursors in fig. 8.

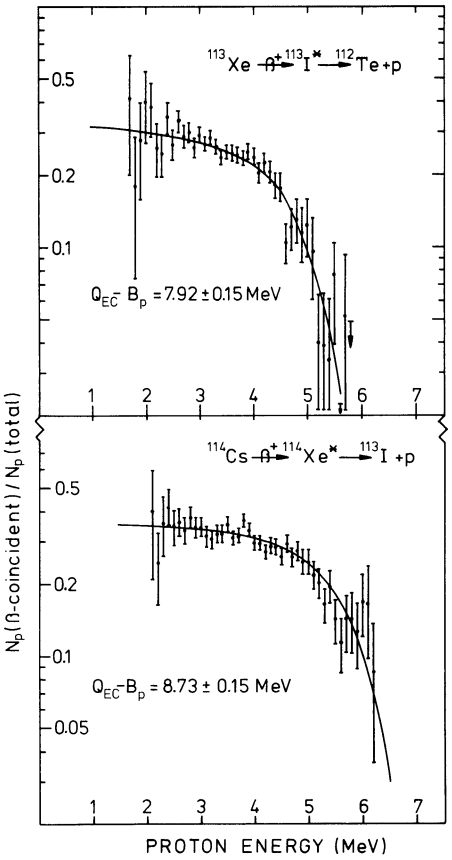

Fig. 8 Intensity ratio of protons measured with and without the requirement of coincident positron detection for the precursors ^{113}Xe and ^{114}Cs. The experimental points have not been corrected for the efficiency of the beta counter (∿35%), which instead was included into the calculated curves. The full-drawn curves represent the best possible fits to the data, taking feeding of excited levels by the proton emission into account, and yielded the energy values given in the figure .

Also shown are the corresponding curves resulting from statistical-model [7] calculations. Treating the $Q_{EC} - B_p$ value as a parameter, such calculations were performed until the best possible agreement with the experimental data was reached. This procedure is necessary, because the feeding of excited levels after the proton emission demolishes the one-to-one relationship of proton energy available for the preceding beta decay. For the ^{114}Cs decay these final states are , as earlier mentioned, not known. We have, therefore, varied the number, energies and spins of the assumed final states in order to see the influence on the derivation of the energy parameter, and included this in the uncertainty on the final result. The resulting $Q_{EC} - B_p$ values are given in table 4, while the masses and proton-binding energies B_p derived from these measurements are treated in a parallel contribution to these proceedings [4].

Table 4

Experimentally determined $Q_{EC} - B_p$ values

Precursor	$Q_{EC} - B_p$, MeV
^{113}Xe	7.92 ± 0.15
^{114}Cs	8.73 ± 0.15

6. Comparison of experimental and calculated data: an indication of a beta-strength resonance in the decays of $^{110,112}I$, ^{113}Xe, $^{114,116}Cs$ and ^{117}Ba.

Following the studies [21] of ^{114}Cs for which a resonance in the underlying beta-strength function [5-7] was proposed, we have undertaken a more systematic investigation of this phenomenon in this mass region. The derivation of information on nuclear properties from experimental data followed the conventional procedure of comparing the measured particle spectra, branching ratios etc. with the corresponding values from statistical model [7] calculations. The most conspicuous deviation was noticed between the measured and calculated particle spectra: in analogy to what was reported[21] for ^{114}Cs, the most neutron-deficient precursors of iodine, xenon and barium all showed experimental spectra having their intensity maxima at energies which were 0.7 - 1.5 MeV higher than those of the corresponding spectra obtained from calculations with standard parameters. As an example, fig. 9 shows the experimental particle spectra of ^{113}Xe together with two calculated sets. It is evident that especially the proton spectrum calculated using a constant beta-strength function and uncorrected level widths is far from being in agreement with the experimental one. This result deviates essentially from most of the results reported earlier (see e.g. the review in ref. [7]).

Because of the large number of parameters entering the statistical-model calculations, it is not possible directly to pick out one quantity as being responsible for the disagreement. We have therefore chosen to make not too violent changes of the parameters and study the influence of such variations.

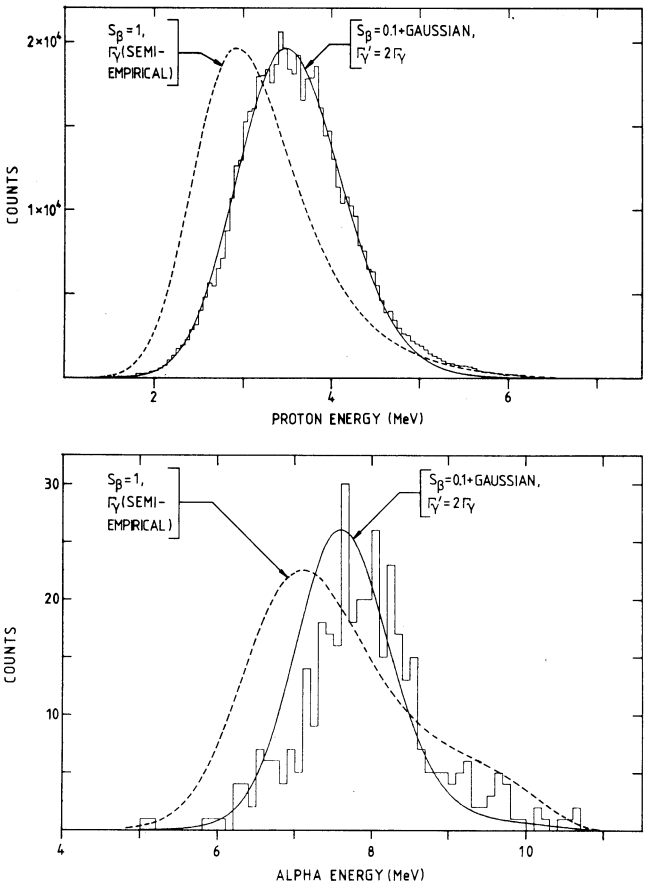

Fig. 9 Experimental (histograms) and calculated (smooth curves) spectra of beta-delayed protons (top) and alpha particles (bottom) of the precursor ^{113}Xe. The intensities correspond to counts per 50 keV and 100 keV for protons and alpha particles, respectively. The two sets of theoretical spectra are based on a spin-parity assignment of $5/2^+$ for ^{113}Xe and the following beta-strength functions: $S_\beta = 1$ (I) and $S_\beta = 0.1 + 2.5 \cdot (0.7 \cdot \sqrt{2\pi})^{-1} \cdot \exp(-(E-5.65)^2/(2 \cdot 0.7^2))$ MeV^{-1} (II), with E being the excitation energy in the beta-decay daughter in MeV. In addition the gamma-emission width was assumed to be equal to the prediction of Cameron[30] in (I), whereas in (II) the predicted values have been multiplied by a factor of two. More details concerning the calculations are given in the text.

Although the $Q_{EC} - B_p$ values are known for several of the cases treated here (refs. [7,31] and this work), we have also varied this quantity. However, in contrast to what might be expected, this brings only minor changes in the position of the maxima of the calculated spectra, when the energy parameters are kept within the limits of various mass predictions [3]; far more is the high-energy tail of the spectra influenced. Hence, the level densities and the partial level widths of the intermediate nuclei and the beta strength of the precursors are left as possible candidates.

Based on particle X-ray coincidence (PXCT) measurements it has been suggested[32-34] that extrapolation of gamma-ray widths Γ_γ, e.g. using the formula of Cameron[30], to the region of very neutron-

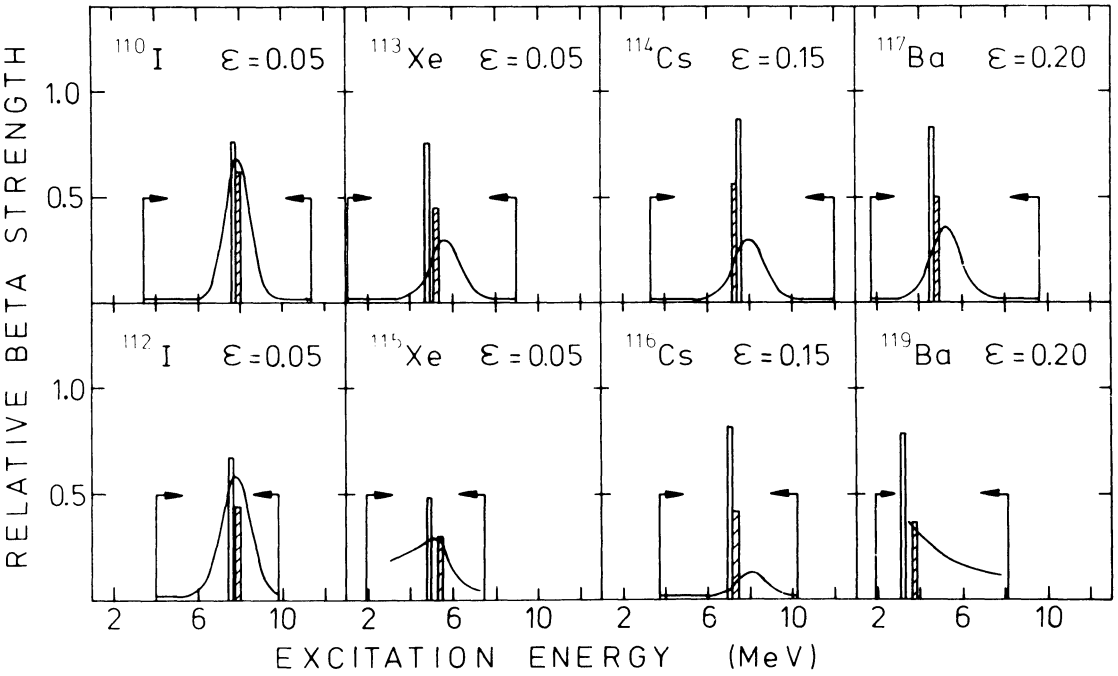

Fig. 10 Beta strengths for eight beta-delayed particle precursors in the A ∼ 115 mass region. The vertical bars represent the $^{7/2}[413]_{\pi} \rightarrow {}^{5/2}[413]_{\nu}$ (hatched) and $^{9/2}[404]_{\pi} \rightarrow {}^{7/2}[404]_{\nu}$ transitions as calculated within the Nilsson model including pairing. The height is giving the intensity obtained as the product of the occupation coefficients V_p^2 and U_n^2. The smooth curves for $^{110,112}I$, ^{113}Xe, $^{114,116}Cs$ and ^{117}Ba are the strength functions offering the best agreement with the experimental spectra as described in the text. It should be mentioned that for ^{113}Xe and ^{114}Cs the gamma-emission width has been multiplied by a factor of two, whereas for the remaining the values resulting from direct application of the Cameron formula [30] were applied. For ^{115}Xe the beta strength was taken from ref. [6], while for ^{119}Ba the curve presents a smooth version of the $S_\beta \cong I_p(exp)/I_p(calc)$ ratio of ref. [31]. The vertical lines with the arrows indicate the region of excitation energy available for investigations by beta-delayed proton spectroscopy: $B_p < E < Q_{EC}$.

deficient nuclides results in too low values. In analogy to the procedure in ref. [32] we have therefore introduced a multiplicative correction factor to Γ_γ^1, but it emerged that factors far outside the limits proposed by the PXCT results were needed to shift the calculated spectra to the experimentally observed positions, and in addition such corrections were accompanied by substantial reductions in the total branching ratios, which in most cases agreed reasonably well when unaltered gamma widths were applied. Therefore, also the level density, which enters the expression [7] for the reduced level width for proton emission, has been varied, again following the pattern outlined in ref. [32]. Even a combination of the two effects appeared not to suffice; for ^{114}Cs, e.g., an enhancement of Γ_γ^1 and of the level-density parameter a of the formula of Gilbert and Cameron [35,36] by factors of 10 and 1.33, respectively, brought the proton spectrum only about two thirds of the way to agreement with the experimental one, and resulted in a reduction of the calculated proton-branching ratio from $4.1 \cdot 10^{-2}$ (in satisfactory agreement with the value $(7 \pm 2) \cdot 10^{-2}$ determined experimentally) to $2.1 \cdot 10^{-3}$.

We have therefore eventually focussed our attention onto the effect of the beta-strength function S_β, which initially was kept constant. It has earlier been reported [6,21,23,31] that in some cases the introduction of a structure in S_β lead to improved agreement between calculated and measured particle spectra, and such resonances were furthermore supported by theoretical arguments [37-39]. We have tentatively added a Gaussian structure to the constant S_β and varied the parameters of the Gaussian to obtain the best possible agreement with the experimental spectra.

Parallel calculations, on which more details will be presented elsewhere[8], performed within a Nilsson model including pairing, yielded positions and relative strengths of allowed unhindered beta transitions. In the relevant mass region only two such transitions, both originating from the paired system of nucleons, can contribute essentially to a beta-strength resonance: $\pi(^{7}/2+[413]) \rightarrow \nu(^{5}/2+[413])$ and $\pi(^{9}/2+[404]) \rightarrow \nu(^{7}/2+[404])$. The intensities of these transitions were found to be 20-50 times stronger than those of the allowed hindered transitions. The initial proton states and the final neutron states originate from the $g_{9/2}$ and $g_{7/2}$ orbitals, respectively. In fig. 10 we show for eight known precursors the strength and position of the unhindered transitions together with the S_β functions derived as described above in the cases investigated here, and taken from ref. [6] for ^{115}Xe and ref. [31] for ^{119}Ba. The general agreement between the calculated and the derived beta-strength resonances is taken as support for the interpretation outlined above, but it must be emphasized, that the best overall agreement is achieved by the simultaneous introduction of beta-strength resonances and a moderate enhancement of the gamma-emission level widths.

7. Conclusions

The experiments described here have a double character. For the elements above tin essentially all measurements which are possible on beta-delayed particle emission with the present production rates have been performed. They have proven to yield much information on the nuclides involved, but still it would be desirable to have more information available on spins, excited levels etc. in the analysis of the data. In contrast to this, the precursors just below tin represent largely a new area, which could be the source of additional information on the nuclides lying on or very near the closed N = 50 shell. In conclusion we find that beta-delayed particle spectroscopy is an extremely useful tool in the study of very neutron-deficient nuclei.

Acknowledgments

The participation of Drs. J. C. Hardy, B. Jonson, S. Mattsson, E. Nolte and G. Nyman in parts of the studies described here is highly appreciated. We also wish to thank C. Bruske, K. H. Burkard and W. Hüller for excellent operation and development of the GSI mass separator and the UNILAC operating group for delivering high-quality ^{40}Ca and ^{58}Ni beams.

References

1) V. A. Karnaukhov, G. M. Ter-Akopyan and V. G. Subbotin, JINR-Preprint P-1070, Dubna, 1962 and Proc. 3rd Intern. Conf. on Reactions between Complex Nuclei, Pacific Grove, USA, 1963, p. 434.

2) R. Barton, R. Mc Pherson, R. E. Bell, W. R. Frisken, W. T. Link and R. B. Moore, Can. J. Phys. 41 (1963) 2007.

3) 1975 Mass Predictions, S. Maripuu (ed.) Atomic Data and Nucl. Data Tables 17 (1976) 411.

4) A. Płochocki, J. Żylicz, R. Kirchner, O. Klepper, E. Roeckl, P. Tidemand-Petersson, I. S. Grant, P. Misaelides and W. D. Schmidt-Ott, these proceedings and to be published.

5) P. G. Hansen, Adv. in Nucl. Phys. 7 (1973) 159.

6) P. Hornshøj, K. Wilsky, P. G. Hansen, B. Jonson and O. B. Nielsen. Nuclear Phys. A187 (1972) 609.

7) B. Jonson, E. Hagberg, P. G. Hansen, P. Hornshøj and P. Tidemand-Petersson, Proc. 3rd Intern. Conf. on Nuclei far from Stability, Cargèse, France, 1976, CERN 76 - 13 (1976) p. 277.

8) P. Tidemand-Petersson, O. Klepper, A. Płochocki, E. Roeckl, D. Schardt and J. Żylicz; to be submitted to Phys. Letters B.

9) C. Bruske, K. H. Burkard, W. Hüller, R. Kirchner, O. Klepper and E. Roeckl, Nucl. Instr. Methods (in press).

10) R. Kirchner, K. H. Burkard, W. Hüller and O. Klepper, Nucl. Instr. Methods (in press).

11) Experiment performed by a GSI-Geneva-Göttingen-München collaboration. O. Klepper et al. ; to be published.

12) E. Nolte and H. Hick, Phys. Letters 97B (1980) 55 and these proceedings.

13) J. Cerny and J. C. Hardy, Ann. Rev. Nucl. Sci. 27 (1977) 333.

14) T. Elmroth, E. Hagberg, P. G. Hansen, J. C. Hardy, B. Jonson, H. L. Ravn and P. Tidemand-Petersson, Nuclear Phys. A304 (1978) 493.

15) W. Reisdorf, GSI-preprint and submitted to Z. Phys. (1981).

16) P. Tidemand-Petersson, R. Kirchner, O. Klepper, W. Kurcewicz, E. Roeckl and E. F. Zganjar; submitted to Z. Phys. A (1981).

17) K. Takahashi, M. Yamada and T. Kondoh, Atomic Data Nucl. Data Tables 12 (1973) 101.

18) D. Schardt, R. Kirchner, O. Klepper, W. Reisdorf, E. Roeckl, P. Tidemand-Petersson, G. T. Ewan, E. Hagberg, B. Jonson, S. Mattsson and G. Nyman, Nuclear Phys. A326 (1979) 65.

19) D. Schardt, T. Batsch, R. Kirchner, O. Klepper, W. Kurcewicz, E. Roeckl and P. Tidemand-Petersson; Nuclear Phys. A (in press).

20) D. Schardt, T. Batsch, R. Kirchner, O. Klepper, W. Kurcewicz, G. Nyman, E. Roeckl, P. Tidemand-Petersson and U. J. Schrewe; these proceedings.

21) E. Roeckl, G. M. Gowdy, R. Kirchner, O. Klepper, A. Piotrowski, A. Płochocki, W. Reisdorf, P. Tidemand-Petersson, J. Żylicz, D. Schardt, G. Nyman and W. Lindenzweig, Z. Phys. A294 (1980) 221.

22) R. Kirchner, O. Klepper, G. Nyman, W. Reisdorf, E. Roeckl, D. Schardt, N. Kaffrell, P. Peuser and K. Schneeweiss, Phys. Letters 70B (1977) 150

23) D. D. Bogdanov, V. A. Karnaukhov and L. A. Petrov, Sov. J. Nucl. Phys. 18 (1974) 1.

24) V. A. Karnaukhov, G. M. Ter-Akopyan, L. S. Vertogradov and L. A. Petrov, Sov. J. Nucl. Phys. 4 (1966) 327.

25) D. D. Bogdanov, V. A. Karnaukhov and L. A. Petrov, Sov. J. Nucl. Phys. 17 (1973) 233.

26) G. M. Gowdy, R. Kirchner, O. Klepper, G. Nyman, W. Reisdorf, E. Roeckl, N. Kaffrell, K. Schneeweiss and D. Schardt; to be published.

27) Table of Isotopes, C. M. Lederer and V. S. Shirley (eds.) 7th edition, J. Wiley and Sons, New York, 1978.

28) I. Bacso, D. D. Bogdanov, S. Daroczsy, V. A. Karnaukhov and L. A. Petrov, Sov. J. Nucl. Phys. 7 (1968) 689.

29) M. G. Johnston, I. S. Grant, P. Misaelides, P. J. Nolan, P. Peuser, R. Kirchner, O. Klepper, E. Roeckl and P. Tidemand-Petersson, these proceedings and to be published.

30) A. G. W. Cameron, Can. J. Phys. 35 (1957) 666.

31) D. D. Bogdanov, A. V. Demyanov, V. A. Karnaukhov, L. A. Petrov and J. Vobořil, Nuclear Phys. A303 (1978) 145.

32) P. Asboe-Hansen, E. Hagberg, P. G. Hansen, J. C. Hardy, B. Jonson and S. Mattsson, Nuclear Phys. A361 (1981) 23.

33) J. C. Hardy, these proceedings.

34) J. C. Hardy et al., to be published.

35) A. Gilbert and A. G. W. Cameron, Can. J. Phys. 43 (1965) 1446.

36) J. W. Truran, A. G. W. Cameron and E. Hilf, Proc. Internat. Conf. on the Properties of Nuclei far from the Region of Beta Stability, Leysin, 1970, CERN 70 - 30 , p. 275.

37) P. O. Martinsen and J. Randrup, Nuclear Phys. A195 (1972) 26.

38) S. P. Ivanova, A. A. Kuliev and Dzh. I. Salamov, Sov. J. Nucl. Phys. 24 (1976) 145.

39) A. A. Bykov and Yu. V. Naumov, Bull. Acad. Sci. USSR, Phys. Ser. 42 (1979) 100.